行政院國家科學委員會專題研究計畫成果報告

克爾效應鎖模雷射之非線性動力學研究

Studies on Nonlinear Dynamics of Kerr-Lens Mode-Locking Lasers

計畫編號：NSC 89-2112-M009-026
執行期限：88 年 8 月 1 日至 89 年 7 月 31 日
主持人：謝文峰教授　　國立交通大學光電工程研究所

一、中文摘要

我們理論決定共振腔結構相關之非線性雷射動力學，並在考慮時空偶合以克爾鎖模雷射腔為例數值模擬確定此理論預測。我們發現週期二、週期三和週期四將發生在特殊架構分別具有 G_1G_2= 1/2, 1/4 (or 3/4) and $\frac{2\pm\sqrt{2}}{4}$ 的條件下。當增加非線性效應，雷射將發展成渾沌。

關鍵詞：非線性動力學、高斯光、克爾效應和雷射

Abstract

We determined theoretically that the nonlinear dynamics of a Gaussian beam is configuration dependent and is confirmed numerically in a Kerr-lens mode-locked cavity in both spatial and temporal domains. Period doubling, tripling and quadrupling can occur in the configurations with G_1G_2= 1/2, 1/4 (or 3/4) and $\frac{2\pm\sqrt{2}}{4}$, respectively, and will become irregular if the nonlinear effect is further increased.

Keywords: nonlinear dynamics, Guassian beam, Kerr effect and laser

二、緣由與目的

After the discovery of KLM in Ti:sapphire laser,[1] various numerically and analytically[2-6] theoretical studies were dedicated to the KLM cavity design. Since a femtosecond pulse will simultaneously undergo self-amplitude (SAM) and self-phase (SPM) modulations as it propagates through a Kerr medium. One may model this problem by preserving the total pulse energy at that moment.[7-8]

Recently, period doubling in a Ti:sapphire laser had been observed near the edge of the stable region and explained in terms of total mode locking[9] and a detailed study about subharmonic oscillations by total mode locking was reported in Ref. 10. The dynamical behavior based on the propagation of single Gaussian beam had been numerically investigated[11] in which the regular, quasi-period and chaotic behaviors were reported in a KLM laser having its configuration close to the limit of stable region that was supported by observation of quasi-period and chaotic behavior in a ring Ti:sapphire laser.[12]

According to our previous theoretical prediction[13] based on the Greene's residue theorem,[14] some specific configurations within the geometrically stable region[15] are very sensitive to the nonlinear effect. We present, in this report, the cavity configuration dependent dynamical behavior of the KLM lasers by modeling the nonlinear dynamics of single Gaussian mode propagation. The result is different from that of totally mode-locking both transverse and longitudinal modes.

三、理論分析與結果

1. Stability of a general lossless cavity

As described in our last year's report or Ref. 15, we have the iterative map of a

Gaussian beam propagation, with the complex beam parameter, relating the q-parameter of the (n+1)-th round-trip to the n-th as[15]

$$w_{n+1} = f_w(w_n, R_n) = \left\{ -\frac{\lambda}{\pi} \mathrm{Im}\left[\frac{C + D(1/R_n - i\lambda/\pi w^2)}{A + B(1/R_n - i\lambda/\pi w^2)} \right] \right\}^{-1/2} \quad (1)$$

and

$$R_{n+1} = f_R(w_n, R_n) = \left\{ \mathrm{Re}\left[\frac{C + D(1/R_n - i\lambda/\pi w^2)}{A + B(1/R_n - i\lambda/\pi w^2)} \right] \right\}^{-1}. \quad (2)$$

This forms a two-dimensional iterative map. Here λ the central wavelength, R the phase-front radius of curvature, w is the spot size of beam, and the round- trip matrix of the cavity of interest is $\begin{bmatrix} A & B \\ C & D \end{bmatrix}$. If all of the elements of ABCD matrix are real (a lossless cavity), this map belongs to a conservative one.[17] Since the fixed point of the map is its self-consistent solution, to determine the characteristics of cavity beam is to discuss the stability of the fixed point through the Greene's residue theorem[13] to define the residue as

$$\mathrm{Re}\, s = \frac{1}{4}\left[2 - Tr(M_J)\right]. \quad (3)$$

Here M_J is the Jacobian matrix of the map and $Tr(M_J)$ is its trace. The relation between residue and the phase shift, θ, of the map per iteration can be represented as[13]

$$\mathrm{Re}\, s = \sin^2(\theta/2). \quad (4)$$

Thus, the residue of a lossless cavity is[12]

$$\mathrm{Re}\, s = 1 - (2G_1G_2 - 1)^2. \quad (5)$$

Here $G_{1,2} = a - b/\rho_{1,2}$ represent the G-parameters of a general optical cavities, $\begin{bmatrix} a & b \\ c & d \end{bmatrix}$ is the transfer matrix of one-way pass between the two end mirrors, and ρ_1 and ρ_2 are the radii of curvature of the two end mirrors, respectively.

From the residue theorem, the fixed point is stable as 0<Res<1; whereas, it is unstable as Res<0 or Res>1. And from Eq. (5), we found the region with $0 < G_1G_2 < 1$ is stable and the regions with $G_1G_2 < 0$ and $G_1G_2 > 1$ are unstable. This result is the same as the geometrically stable one.[14] Besides the Res=0 and 1 are critical, the residue theorem proposes that the orbit is stable for 0<Res<1 except for Res=3/4 and sometimes 1/2. These special cases with Res=0, 1, 3/4 and 1/2 correspond to the low order resonance where $\chi^p=1$ having p=1, 2, 3 and 4, respectively. Here χ is the eigenvalue of the M_J. These special conditions correspond to $G_1G_2=0$ or $G_1G_2=1$ for Res=0, $G_1G_2=1/2$ for Res=1, $G_1G_2=1/4$ or 3/4 for Res=3/4 and $G_1G_2 = \frac{2 \pm \sqrt{2}}{4}$ for Res=1/2, respectively. In Fig. 1, the diagram of stable region is shown with the dashed curves representing these critical configurations.

2. Kerr-lens mode-locked cavity

The KLM cavity is the same as in Ref. 20. Analyzing propagation of Gaussian beam through that the ABCD law is applied for linear optical components and the renormalized q-parameter's method[8,14] is used in Kerr medium. Let the reference plane be where the beam just leaving the end-mirror. By cascading the propagation of q-parameter in a round trip, the complicated transformation of q-parameter relating the (n+1)-th to the n-th round trip forms a two-dimensional iterative map as

$$w_{n+1} = f_w(R_n, w_n; K) \quad (6)$$

and

$$R_{n+1} = f_R(R_n, w_n; K). \quad (7)$$

We label the map as $\boldsymbol{Q}_{n+1} = \boldsymbol{F}_K(\boldsymbol{Q}_n)$, where $\boldsymbol{Q}_n = \begin{bmatrix} w_n \\ R_n \end{bmatrix}$ and n represents the iterative number. The Kerr parameter K corresponds to the nonlinear parameter.

By constraining K to less than 0.4 in simulation because the steady-state K value is usually greater than 0.4 in the experimental results as in Ref. 19. Because the similar

dynamical behavior occurs in sagittal and tangential planes, we will concentrate the simulations on the sagittal plane only. The two adjustable variables are z and r_1, where z is the separation of the two curved mirrors and r_1 the distance between the curved mirror M_2 and the rod endface I. The z value mainly determines the geometrically stable region, and r_1 affects the efficiency of Kerr effect.

Table 1 lists the configurations and z values corresponding to low order resonance at K=0 and types of bifurcations. Since there are two stable regions, each G_1G_2 will have two z values.

When z=113.34mm, the configuration is near G_1G_2=1/2, we found period-doubling bifurcation in spot size when the nonlinear parameter K increases. The period-2 fixed point, $\boldsymbol{Q}_2$, is the solutions of $\boldsymbol{F}_K(\boldsymbol{F}_K(\boldsymbol{Q}_2))-\boldsymbol{Q}_2=0$. It is clear that $\boldsymbol{Q}_2$ represents the self-consistent Gaussian beam of two round trips. The critical K, at which transition from period one to period doubling takes place approximately at K_c=0.0008353. There is only one stable period-1 solution as $K<K_c$; whereas, a pair of stable period-2 fixed points exist and the period-1 fixed point becomes separatrix in phase space as $K>K_c$.[21]

In fact, the Poincare-Birkhoff theorem tells us that some of period-2 fixed points survive if a nonlinear term is added to perturb the critical stable system having Res=1.[23] Apparently, this theorem governs the simulation results that the configurations near G_1G_2=1/2 develop to the period doubling as the existence of nonlinear effect. Because the self-focusing causes the equivalent configuration to change, the configuration near G_1G_2=1/2 can also occur period doubling bifurcation. The region of the existence of period doubling is about 60 μm for z. And under different z it ranges from several to tens of millimeters for r_1. Moreover, the intracavity peak power required to reach period doubling decreases and becomes smaller than that of the initial pulse buildup as the configuration approaches to G_1G_2=1/2. From the experimental result of Ref. 22, the initial coherent spike of pulse buildup is about 10-40 ps due to partially phase locking of the longitudinal modes. The calculated K of initial spike for 40 ps is about 0.001 in a KLM laser with the intracavity average power P_{av}=10 W and 100 MHz repetition rate. It implies that the KLM laser operated at this configuration can directly build up a period-doubling pulse train. Nevertheless, the region satisfying such a condition is less than 1 μm for z, and K_c rapidly increases to greater than 0.01 when z is set 10 μm away from G_1G_2=1/2. Thus, it may be not easily in experiment to observe period doubling prior to building up period. Therefore, we believe that period doubling can be observed at the configuration near G_1G_2=1/2. Indeed, very recently we have experimentally confirmed this prediction.

Altering the configuration to nearby G_1G_2=1/4 (or 3/4), period-3 bifurcation happens for Res=3/4 with the average angle of rotation per period $\theta=2\pi/3$. Thus, it is expected to find the period-3 solution of map with the evolution of iteration returns to its initial value after 3 iterations. The fixed points of period 3, $\boldsymbol{Q}_3$, can be obtained from $\boldsymbol{F}_K(\boldsymbol{F}_K(\boldsymbol{F}_K(\boldsymbol{Q}_3)))-\boldsymbol{Q}_3=0$.

Besides the period-3 pulse train can be observed on oscilloscope, we think that the far-field pattern may contain two portions: One has smaller beam size for the solution having beam waist at M_1, the other is an already divergent spot for the solutions without matching boundary condition. Similarly, period 4 exists at the configurations with $G_1G_2=\left(2\pm\sqrt{2}\right)/4$ for Res=1/2. There are two fixed points matching the curvature of M_1 and the other two are without matching it. Table. 1 summarizes the dynamical behaviors for G_1G_2 and z values. The character of nonlinear dynamics depends on the configuration, in particular, is determined by the residue even though the z values are

different.

4. Spatial-temporal analysis of KLM cavity

A spatial-temporal analysis involving the spatial and temporal ABCD matrices has been used to transform a Gaussian pulse having Gaussian spatial profile to optimize the optical pulse width in KLM laser.[7,8] The Ti:sapphire laser rod has single pass GVD of 1280 fs^2, bandwidth limiting 10 nm and a pair of the Brewster-angle SF10 prisms are separated by 40 cm. The cavity beam propagates through the apexes of both prisms with insertion of 3 mm. A Gaussian aperture is located at the M_1 mirror with diameter of 2 cm. A seeded pulse with initial value $(w_0,R_0,\sigma_0,\eta_0)$ = (0.7mm, ∞,1ps,0), by keeping the total pulse energy be constant during the propagation, the evolution of spatial parameter (w, 1/R) at M_1. Note that the constant total energy assumption is appropriate for Ti:sapphire rod whose gain recovery time is shorter than the round trip time. The evolution of spatial parameter in portrait diagram looks like three spirals and jumps among these spirals with regular order. Eventually, it converges to the centers of spirals. These centers correspond to the period-3 fixed points, which are (w, 1/R) = q_1(1.46mm, 0.94m^{-1}), q_2(1.35mm, -1.04m^{-1}) and q_3(2.71mm, -0.01m^{-1}). Apparently, all the fixed points are no longer matching the curvature of M_1 because the introduced Gaussian aperture (a diffraction loss) makes the system become dissipative. Since space and time couple in the nonlinear medium, the evolution of pulse width also appears period-3 behavior. The pulse width approaches the period-3 solution with σ_1=86.72fs, σ_2=80.76fs and σ_3=110.42fs. Owing to the system automatically converges to period 3, it indicates that the period-3 solution is more stable than the period-1 one even though the period-1 and period-3 steady-state solutions exist simultaneously.

Furthermore, we also took into account the gain guiding in spatial domain by introducing a complex matrix of Gaussian duct.[25] The result is the same as the previous one that the system eventually converges to the period 3, with only faster convergent rate of adding gain-guiding effect.

5. Irregular behavior

The intensity fluctuation versus number of measure is shown in Fig. 2 with K=0.4. For the sake of observing the long-term evolution, each measure of the intensity variation is obtained by averaging over 300 iterations then normalized to the average intensity over all data points. The regular evolution appears in Fig. 2(b) with the initial value (w_0, 1/R)=(0.705mm, 0). Such an evolution corresponds to regular orbit showing as the invariant circle in a conservative map.[21] When the initial spot size varies to w_0=0.71mm, the evolution becomes irregular as shown in Fig. 2(a). This behavior results from that the nonlinear perturbation brings about the breakdown of the separatrix accompanied with creation of the stochastic layer. These initial-condition dependent irregular behaviors belong to the classical chaos[22] which can be predicted from the residue theorem with Res=3/4.

四、結論

We show a typical cavity configuration dependent nonlinear dynamics. From analyzing the iterative map of a general cavity by the Greene's residue theorem, the specific configurations correspond to the product of generalized G-parameters equal to 1/2, 1/4 (or 3/4) and $\frac{2\pm\sqrt{2}}{4}$ located within the geometrically stable region. This result implies that the nonlinear effects may break their stability of self-consistent Gaussian modes derived from linear cold cavity.

When the propagation of fundamental Gaussian beam in KLM cavity, the numerical results confirm period doubling, tripling and quadrupling can be obtained at the above-mentioned configurations and the irregular evolution will develop by increasing the

nonlinear effect. This research gives a useful suggestion to implement laser cavities for studying the nonlinear phenomena of Gaussian mode in general.

五、自我評估

我們成功地以理論決定共振腔結構相關之非線性雷射動力學，並在考慮時空偶合以克爾鎖模雷射腔為例數值模擬確定此理論預測。我們發現在特殊架構下將發生週期二、週期三和週期四及渾沌現象。在實驗上我們也證實 KLM **雷射產生在這些特殊結構及不但觀察到週期二、週期三和週期四及渾沌等現象，也發現及了解諧頻鎖模之機制，正進行數據整理與論文撰寫中，依計劃進度執行。**

六、參考文獻

1. D. E. Spence, P. N. Kean, and W. Sibbett, Opt. Lett. 16, 42-44 (1991).
2. M. Piche, Opt. Commun. 86, 156-160 (1991).
3. G. W. Pearson, C. Radzewicz, and J. S. Krasinski, Opt. Commun. 94, 221-226 (1992).
4. J. Herrmann, J. Opt. Soc. Am. B. 11, 498-512 (1994).
5. G. Cerullo, S. De Silvestri, V. Magni, and L. Pallaro, Opt. Lett. 19, 807-809 (1994).
6. K.-H. Lin and W.-F. Hsieh, J. Opt. Soc. Am. B. 11, 737-741 (1994).
7. J. L. A. Chilla and O. E. Martinez, J. Opt. Soc. Am. B. 10, 638-643 (1993).
8. K.-H. Lin and W.-F. Hsieh, 13, 1786-1793 (1996).
9. D. Cote and H. M. van Driel, Opt. Lett. 23, 715-717 (1998).
10. S. R. Bolton, R. A. Jenks, C. N. Elkinton, and G. Sucha, J. Opt. Soc. Am. B. 16, 339-344 (1999).
11. V. L. Kalashnikov, I. G. Poloyko, and V. P. Mikhailov, J. Opt. Soc. Am. B. 14, 2691-2695 (1997).
12. Q. Xing, L. Chai, W. Zhang, and C. Wang, Opt. Commun. 162, 71-74 (1999).
13. M.-D. Wei , W.-F. Hsieh, and C. C. Sung, Opt. Commun. 146, 201-207 (1998).
14. J. M. Greene, J. Matm. Phys. 20, 1183-1201 (1979).
15. A. E. Seigman, *Laser*, Chap.20-21 (University Science, Mill Valley, CA, 1986).
16. H. A. Haus, J. G. Fujimoto, and E. P. Ippen, IEEE J. Quantum Electron. 28, 2086-2096 (1992).
17. L. M. Sanchez and A. A. Hnilo, Opt. Commun. 166, 229-238 (1999).
18. M.-D. Wei, W.-F. Hsieh, and C. C. Sung, Opt. Commun. 155, 406-412 (1998).
19. M. Mechendale, T. R. Nelson, F. G. Omenetto, and W. A. Schroeder, Opt. Commun. 136, 150-159 (2997).
20. B. E. Lemoff and C. P. J. Barty, Opt. Lett. 17, 1367-1369 (1992).
21. K.-H. Lin, Y. Lai, and W.-F. Hsieh, J. Opt. Soc. Am. B. 12, 468-475 (1995).
22. R. S. MacKay, *Renormalisation in Area-preserving Maps*, Chap. 1 (World Scientific, Singapore, 1993).
23. J.-M. Shieh, F. Ganikhanov, K.-H. Lin, W.-F. Hsieh, and C.-L. Pan, J. Opt. Soc. Am. B. 12, 945-949 (1995).
24. A. J. Lichtenberg, and M. A. Lieberman, *Regular and Chaotic Dynamics* (Springer- Verlag, New York,1992) Chap. 3.
25. J.-G. Juang, Y.-C. Chen, S.-H. Hsu, K.-H. Lin, and W.-F. Hsieh, J. Opt. Soc. Am. B, 14, 2116-2121 (1997).
26. F. Salin and J. Squier, Opt. Lett. 17, 1352-1354 (1992).

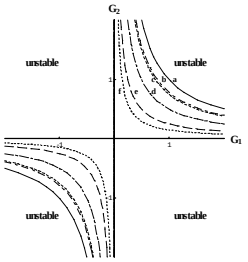

Fig.1

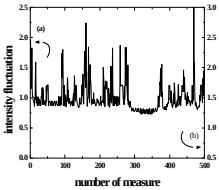

Fig. 2